

Supporting Information

Achieving Dendrite-Free Zn Anode at High Current Densities via In-Situ Polymeric Interface Design

Zhipei Zhong, Wenhao Ren, Suqing Wang*

School of Chemistry & Chemical Engineering, South China University of Technology,
Guangzhou 510640, China

* Corresponding author E-mail: cesqwang@scut.edu.cn (S. Wang).

Experimental Section

Material synthesis

Electrolyte preparation: The reference group electrolyte was 3M ZnCl₂. The test group electrolyte (AM/ZnCl₂ electrolyte) were prepared by adding different amount (0.1, 0.2 and 0.3 M, respectively) of AM and different amount (0.01, 0.02 and 0.03 M, respectively) of N,N-Methylenebisacrylamide (NMAM) into 3 M ZnCl₂ electrolyte.

Synthesis of NVO cathode materials: A simple hydrothermal method is applied to prepare NVO. 1.053 g of commercial NH₄VO₃ powders were added into 45 mL of deionized water. The above solution was completely dissolved at 80°C under continuous magnetic stirring for 1 h. Subsequently, 1.7019 g of H₂C₂O₄ · 2H₂O was added and stirred at room temperature until the color of solution turned to black-green. The obtained solution was poured into a 50 mL Teflon-hydrothermal reactor and heated in an oven at 140°C for 14 h. The NVO powders were collected by vacuum filtration and washing several times with deionized water. Finally, the NVO powers were dried in 80 °C.

Preparation of electrodes and assembly of full cells: The cathode electrodes were fabricated by mixing the NVO materials with super P and polyvinylidene fluoride

(PVDF) with a weight ratio of 7:2:1. The above mixture was mixed in an appropriate amount of N-methyl-2-pyrrolidone (NMP) to form a slurry under vigorously stirring for 5 h, and then spread onto Ti foil, dried in a vacuum oven at 80 °C. The cathode electrode is cut into 12mm discs. The mass loading of the disc was about 2 mg. Symmetric cells and full cells were assembled using Zn foils (14mm) as anodes in Swagelok cells, and 150 μ L of electrolyte (3 M ZnCl₂ or AM/ZnCl₂) was utilized with the glass fiber (Whatman, grade GF/D) as the separator.

Electrochemical testing

The battery performance was evaluated by using Swagelok cells on a LAND battery test system (CT2001A, Wuhan, China). The Zn plating/stripping tests were performed on Zn//Zn symmetrical cells in the electrolytes with and without AM. Coulombic efficiency (CE) measurements were carried out on asymmetrical Zn//Cu cells. The corrosion, diffusion and hydrogen evolution behaviors of Zn foil electrodes were performed by an electrochemical station (Gamry 1010). The Tafel plots were measured by scanning between -0.2 and 0.2 V at 1 mV s⁻¹ by Zn//Zn symmetrical cells. The diffusion curves were recorded by chronoamperometry method under an overpotential of -150 mV by Zn//Zn symmetrical cells. The hydrogen evolution performance was collected through linear sweep voltammetry (LSV) with a potential range of -0.3 ~ 0 V vs. Zn/Zn²⁺ at a scan rate of 1 mV s⁻¹ by Zn//Ti symmetrical cells. Electrochemical impedance spectroscopy (EIS) was implemented within a range of 10⁵ to 10⁻² Hz. The full cells were cycled between 0.4 and 1.4 V vs. Zn/Zn²⁺, and the specific capacities were evaluated according to the mass of active materials. Cyclic voltammetry (CV) test is executed by Electrochemical workstation (Gamry 1010) at room temperature at a scan rate of 0.5 mV s⁻¹ in the voltage between 0.4 to 1.4 V.

Materials characterization

Field emission scanning electron microscope (SEM, Regulus SU8100) was used to characterize morphology. X-ray diffraction (XRD) patterns were obtained on a Bruker D8 advance X-ray diffractometer with Cu-K α radiation ($\lambda = 0.15418$ nm). Atomic force microscopy (AFM) images were acquired in tapping mode using a SPM-9700HT. The Fourier transform infrared (FTIR) (Nicolet IS50-Nicolet Continuum) was used to detect

the presence of PAM on Zn foil. Raman spectroscopy (HJY LabRAM Aramis) was conducted to analysis the component on the surface of the Zn foil after circulation. In-situ optical microscope images were obtained from a YM710R optical microscope. A DataPhysics Micro apparatus (OCA40) was used to study the contact angles. X-ray photoelectron spectroscopy (XPS) testing was performed on an X-ray photoelectron spectrometer (Thermo SCIENTIFIC Nexsa).

Computation methods

DFT calculation method: The first-principles ^{1,2} have been employed to perform all density functional theory (DFT) calculations within the generalized gradient approximation (GGA) using the Perdew-Burke-Ernzerhof (PBE) ³ formulation. We have chosen the projected augmented wave (PAW) potentials ^{4,5} to describe the ionic cores and take valence electrons into account using a plane wave basis set with a kinetic energy cutoff of 450 eV. Partial occupancies of the Kohn-Sham orbitals were allowed using the Gaussian smearing method and a width of 0.05 eV. The electronic energy was considered self-consistent when the energy change was smaller than 10^{-5} eV. A geometry optimization was considered convergent when the energy change was smaller than $0.05 \text{ eV } \text{\AA}^{-1}$. The vacuum spacing in a direction perpendicular to the plane of the structure is 20 \AA for the surfaces. The Brillouin zone integration is performed using $3 \times 3 \times 1$ Monkhorst-Pack k-point sampling for a structure. Finally, the adsorption energies (E_{ads}) were calculated as $E_{\text{ads}} = E_{\text{ad/sub}} - E_{\text{ad}} - E_{\text{sub}}$, where $E_{\text{ad/sub}}$, E_{ad} , and E_{sub} are the total energies of the optimized adsorbate/substrate system, the adsorbate in the structure, and the clean substrate, respectively. And the Binding energies (E_{b}) were calculated as $E_{\text{b}} = E_{\text{total}} - E_{\text{Zn}} - E_{\text{sub}}$, where E_{total} , E_{Zn} , and E_{sub} are the total energies of the binding structures system, the Zn atom in the structure, and H_2O or $\text{C}_3\text{H}_5\text{NO}$ (acrylamide) the clean substrate, respectively. Interface energy is calculated using the $\gamma = (E_{\text{system}} - E_{\text{sub1}} - E_{\text{sub2}}) / A$, where the E_{system} is the interface structures, E_{sub1} , E_{sub2} is the energy of Zn surface and $\text{C}_3\text{H}_5\text{NO}$ structures, A is the area of interface.

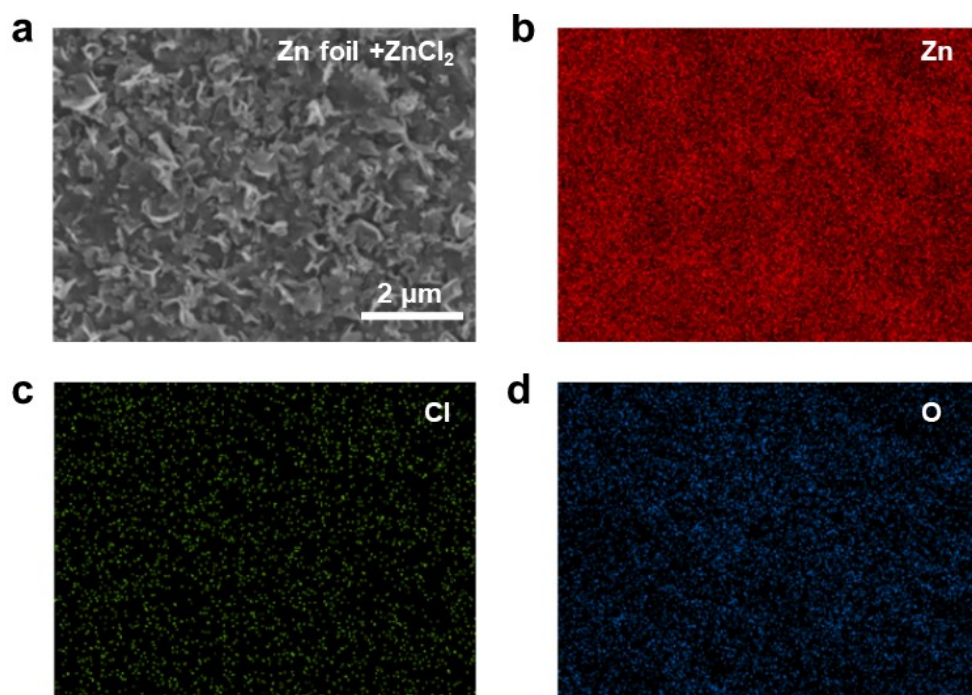


Fig. S1 The SEM image of (a) Zn foil immersed ZnCl₂ electrolyte for 5 days and corresponding EDS analysis results of (b) Zn, (c) O and (d) O element.

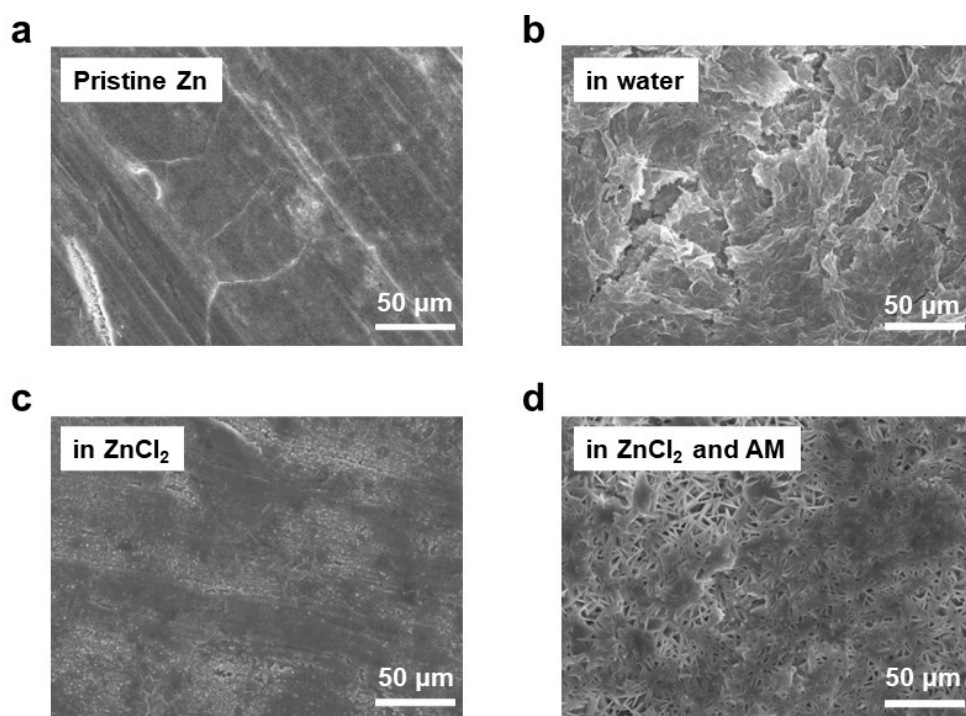


Fig. S2 SEM images of (a) Zn foil at pristine state and immersed into (b) water, (c) ZnCl₂ electrolyte and with (d) AM additive for 5 days.

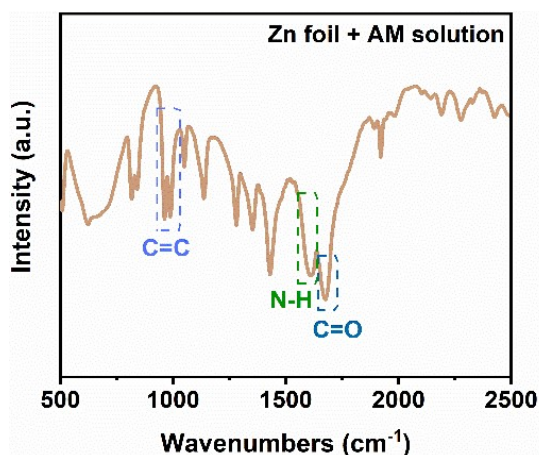


Fig. S3 FTIR spectra of the Zn Foil immersed AM solution.

The peaks of C=O stretching vibration at 1676 cm^{-1} and N-H bending vibration at 1610 cm^{-1} , and the characteristic peak of the C=C bond around 980 cm^{-1} all indicate that the AM will be adsorbed on the Zn foil before polymerization reaction occurs.

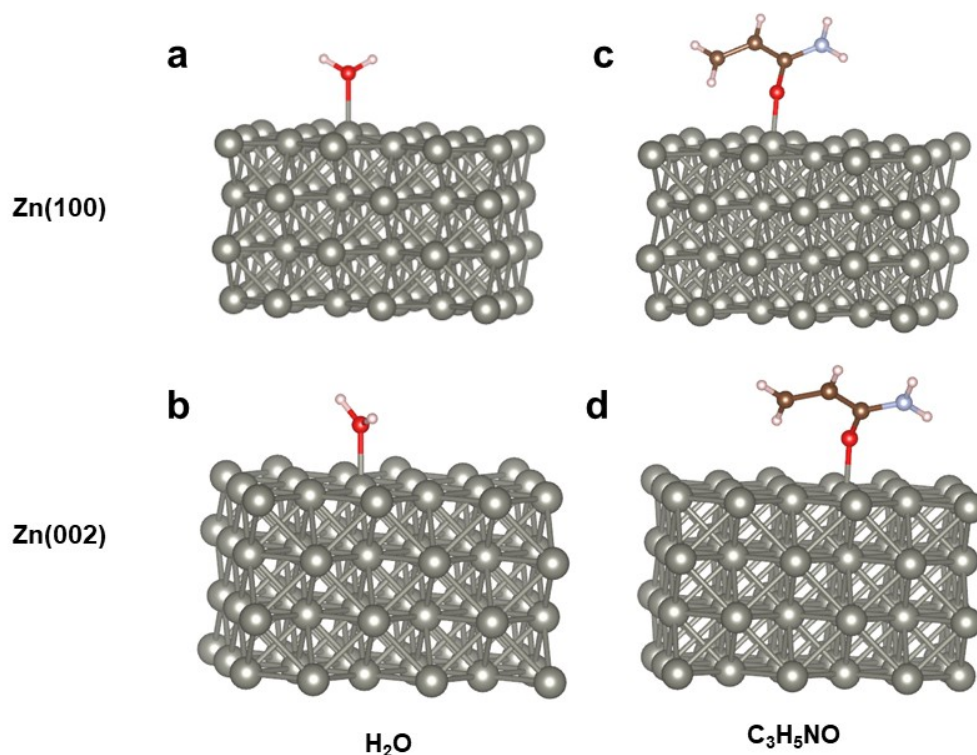


Fig. S4 Structure diagram of (a) H_2O molecule adsorbed on Zn (100) plane, (b) H_2O molecule adsorbed on Zn (002) plane, (c) acrylamide molecule adsorbed on Zn (100) plane and (d) acrylamide molecule adsorbed on Zn (002) plane.

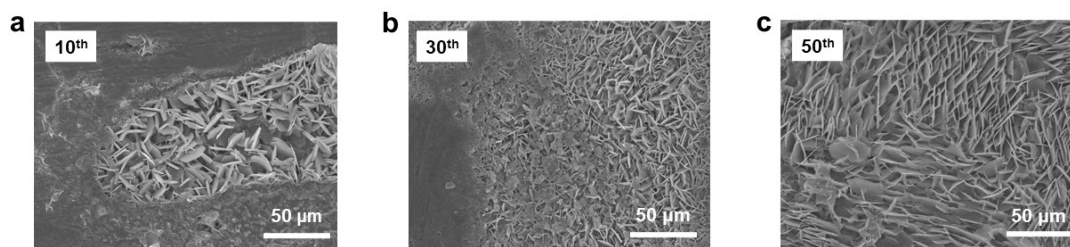


Fig. S5 SEM images of the Zn foil after (a) 10th, (b) 30th and (c) 50th symmetric cycles at 1 mA cm⁻² and 1 mA h cm⁻² in ZnCl₂ electrolyte.

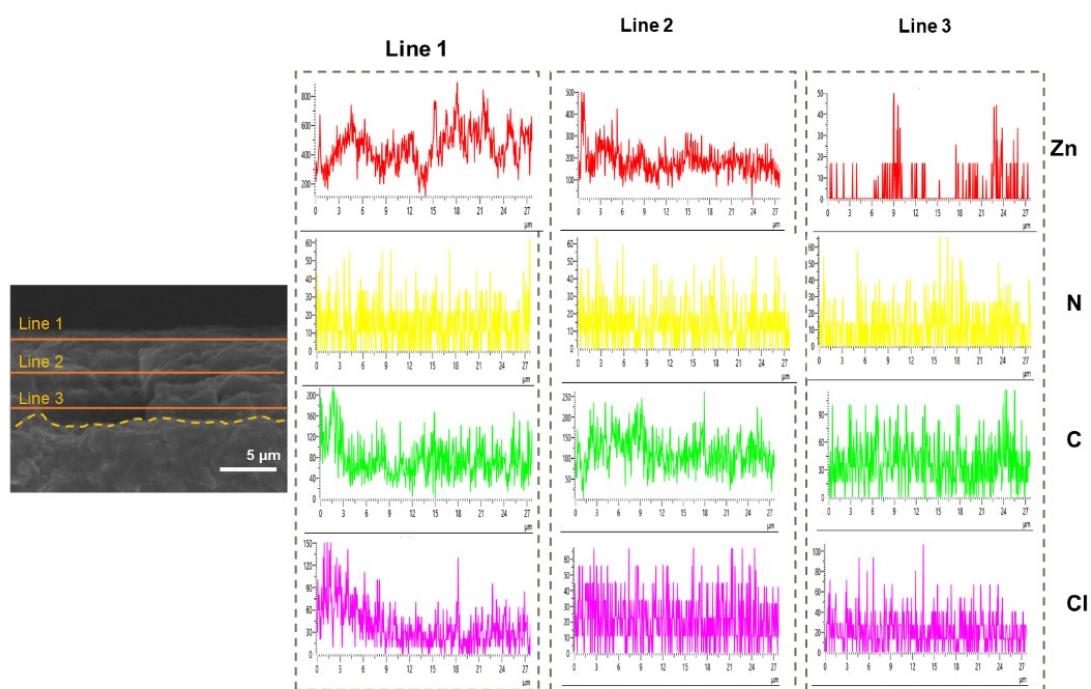


Fig. S6 The line scanning results of EDS analysis in the plating state after 50 cycles.

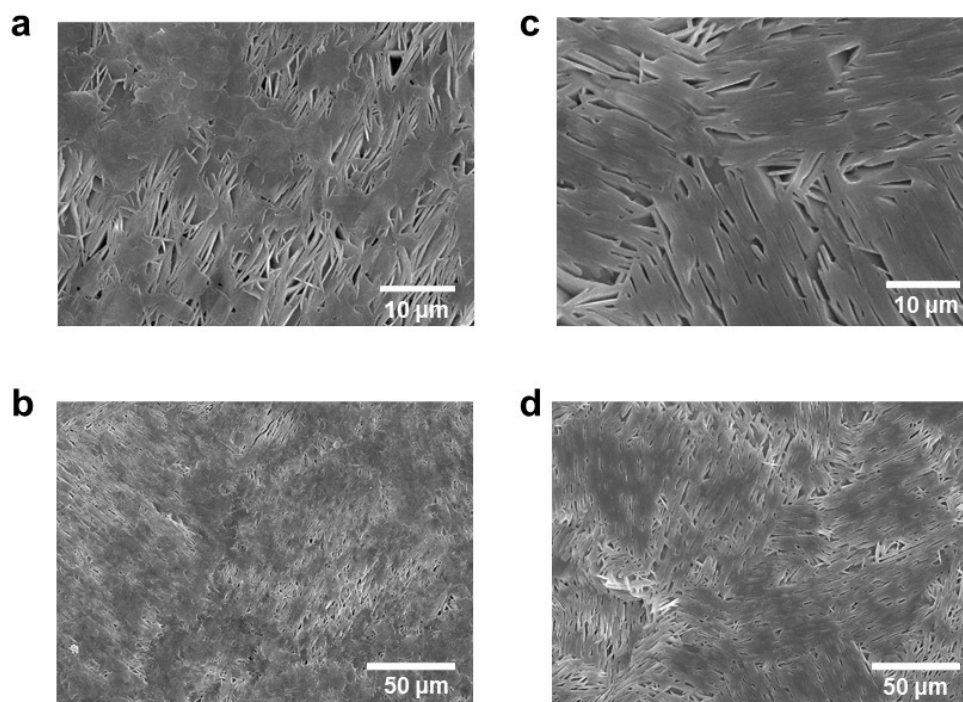


Fig. S7 SEM images of the Zn foil after 650th cycles at (a) (b) plating state and (c) (d) stripping state with AM additive (1 mA cm^{-2} and 1 mA h cm^{-2}).

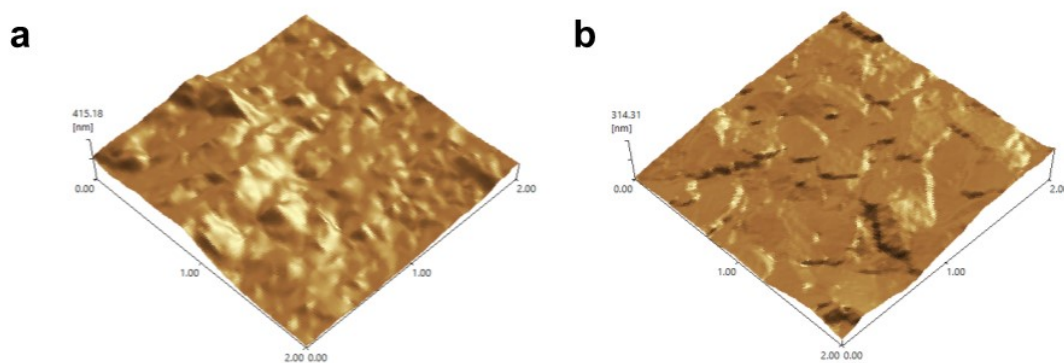


Fig. S8 3D AFM images of Zn metal after 50 cycles in the electrolyte at 1 mA cm^{-2} and 1 mA h cm^{-2} (a) without AM and (b) with AM.

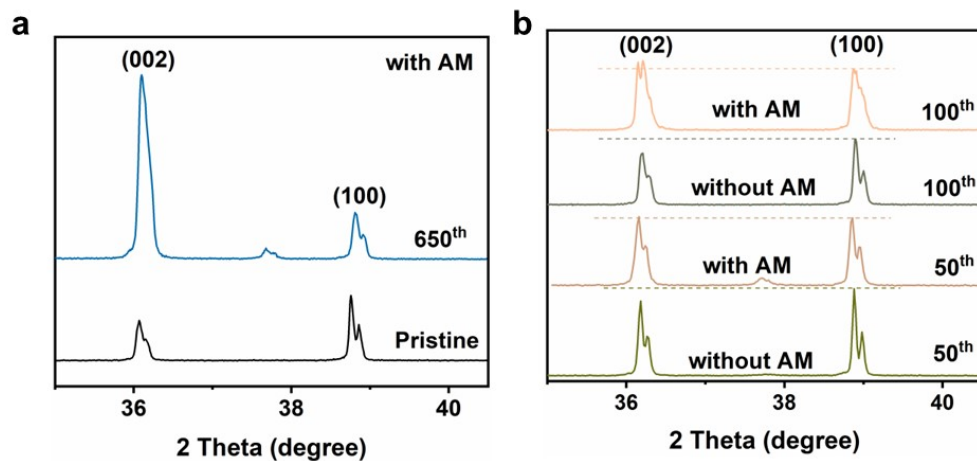


Fig. S9 The XRD patterns of Zn anodes after Zn plating at different cycles with and without AM additive.

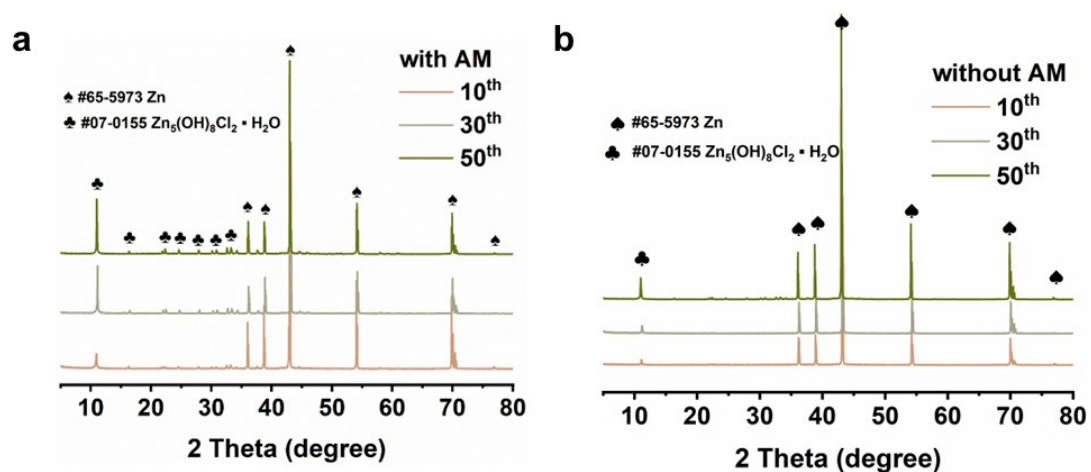


Fig. S10 The XRD patterns of Zn anode after 10th, 30th and 50th cycles at 1 mA cm⁻² and 1 mA h cm⁻² with (a) AM additive and (b) without AM additive.

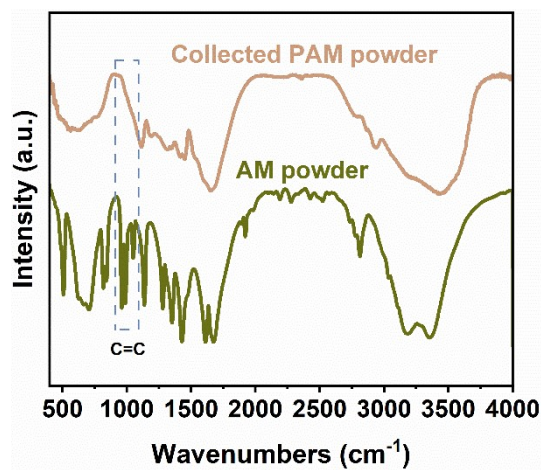


Fig. S11 Comparison of collected PAM powder and AM powder's FTIR spectra.

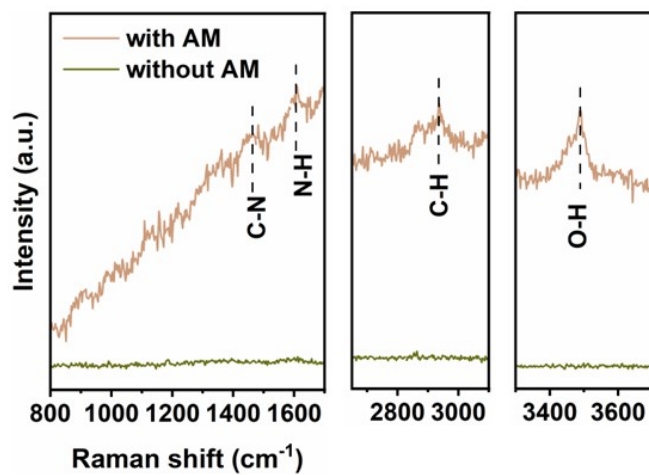


Fig. S12 Raman spectra of cycled Zn anode with and without AM.

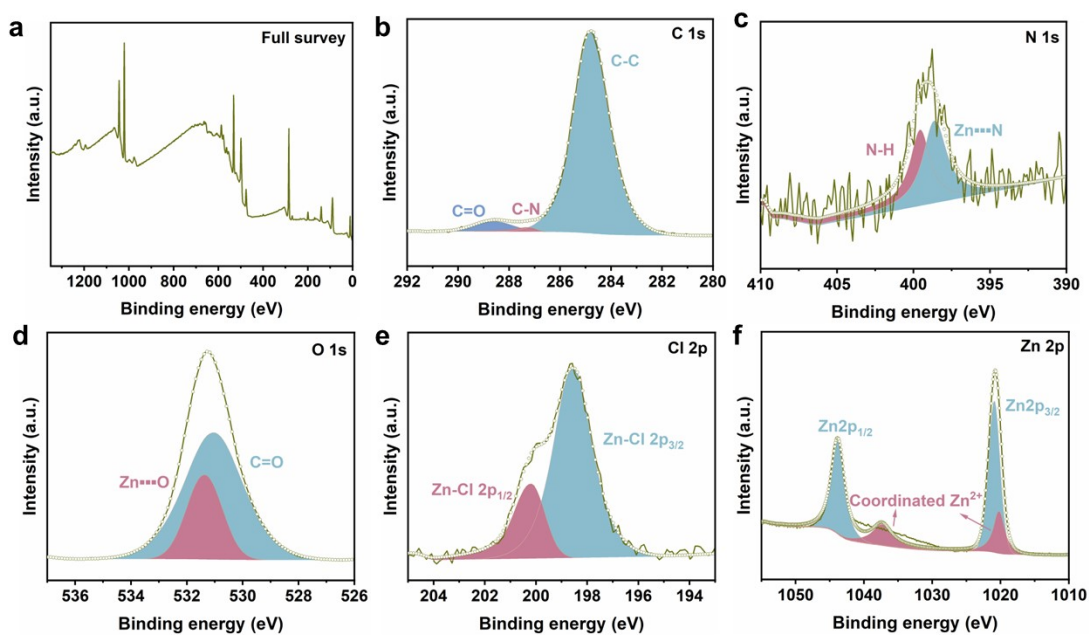


Fig. S13 XPS analysis of (a) full survey, (b) C 1s, (c) N 1s, (d) O 1s, (e) Cl 2p, (f) Zn 2p spectrum of the Zn anode after circulation with the addition of AM additive.

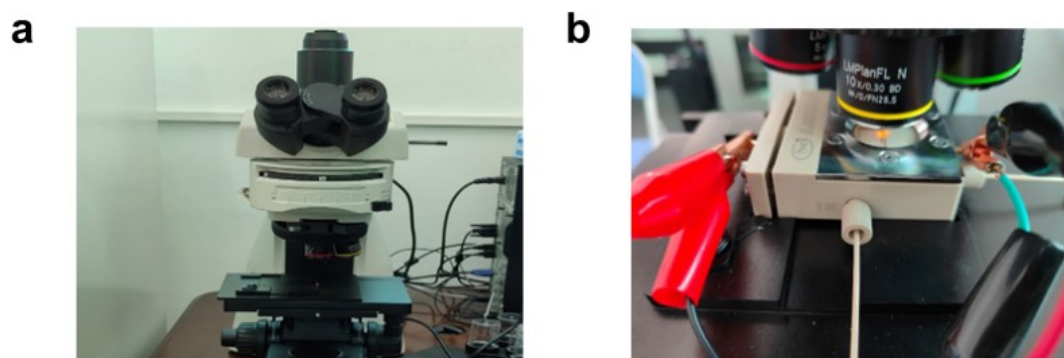


Fig. S14 Optical microscopy (a) and the reaction cell (b) for in-situ observation of the Zn plating process.

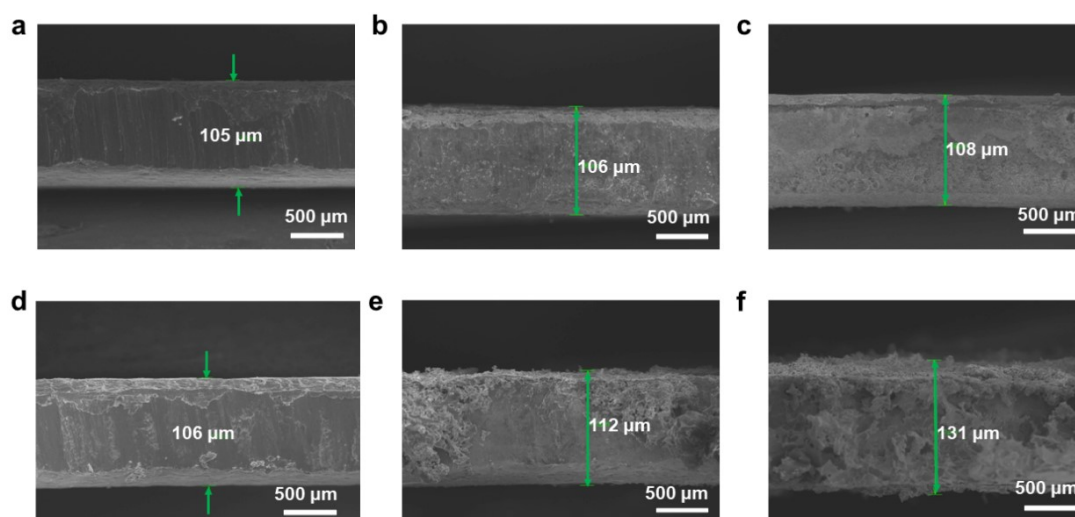


Fig. S15 The cross-section SEM images of Zn anodes with AM additive after (a) 10 cycles, (b) 30 cycles and (c) 50 cycles. The cross-section SEM images of Zn anode without AM additive after (d) 10 cycles, (e) 30 cycles and (f) 50 cycles.

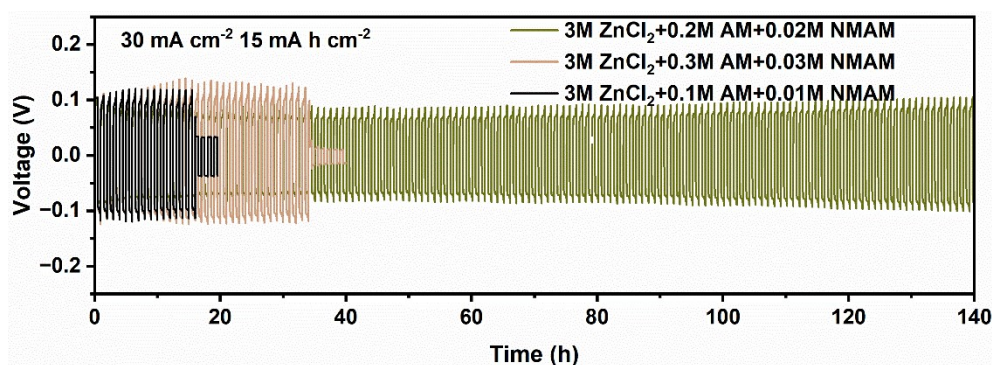


Fig. S16 Effect of AM additive concentration on the performance of symmetrical cells at 30 mA cm^{-2} and 15 mA h cm^{-2} . The result shows that the generated in-situ SEI film is too thin or too thick will have an impact on the performance, so the AM concentration is selected as 0.2 M in the later.

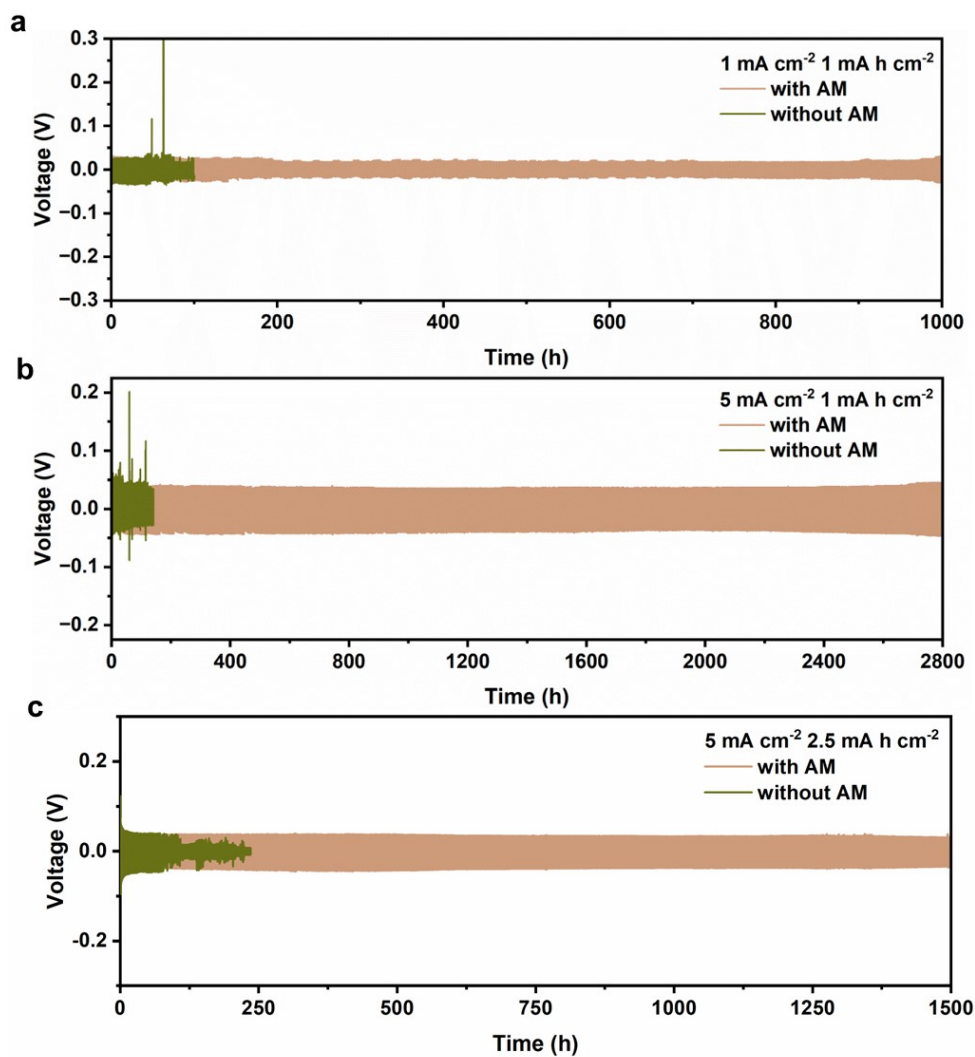


Fig. S17 The performance of Zn//Zn symmetrical cells with and without AM additive at (a) 1 mA cm^{-2} and 1 mA h cm^{-2} , (b) 5 mA cm^{-2} and 1 mA h cm^{-2} , (c) 5 mA cm^{-2} and 2.5 mA h cm^{-2} .

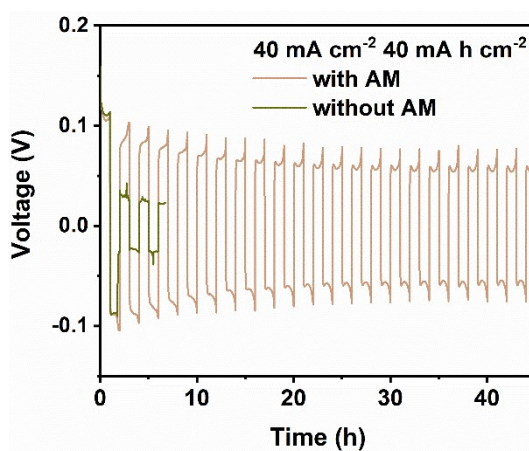


Fig. S18 The performance of Zn//Zn symmetrical cells at 40 mA cm^{-2} and 40 mA h cm^{-2} .

$$Zn_{DOD} = \frac{\text{Actual area capacity (mA h cm}^{-2}\text{)}}{0.585 \times d \text{ (mA h cm}^{-2}\text{)}} \times 100\%$$

d represents Zn foil thickness (μm)

Table S1 the comparison of references with different strategies

Strategy	Current density (mA cm ⁻²)	Specific capacity (mA h cm ⁻²)	Cycles number (n)	Depth of discharge (%)
enamel-like nano-HAP layer ⁶	0.1 10	0.1 5	2400 400	- -
NGDY modified CS separator ⁷	5 10	1 1	500 200	- -
thiourea electrolyte additive ⁸	1 10	1 1	1200 600	1.71% 1.71%
electrochemical pretreatment of Zn electrode ⁹	5 7.5 10	1 1 1	1000 700 500	2.13% 2.13% 2.13%
weighing paper separator interlayer ¹⁰	1 9	1 4.5	2400 800	1.71% 7.69%
amino acid electrolyte additive ¹¹	5 10	4 4	2400 900	- -
3D artificial array electrode ¹²	1 5	1 1.25	1500 800	1.71% 2.14%
xylitol electrolyte additive ¹³	1 5	1 1	1100 1000	5.68% 5.68%
bio-inspired silk fibroin coating ¹⁴	1 10	1 2	1500 500	1.65% 3.30%
interface stabilizer electrolyte additive ¹⁵	2 10	2 2	800 240	- -

ammonium cationic	1	2	1000	2.28%
surfactants electrolyte	2	2	900	2.28%
additive ¹⁶	5	5	600	5.70%
	10	5	500	5.70%
non-aqueous	2	2	1500	-
electrolyte system ¹⁷	3	1	1200	-
	5	1	1200	-
Organic/inorganic	1	1	450	1.71%
hybrid artificial	5	1	1000	1.71%
functional layer ¹⁸	10	1	700	1.71%
This work	5	1	2800	1.71%
	5	2.5	1500	4.27%
	10	5	1400	8.55%
	30	15	140	25.64%
	40	40	45	68.38%

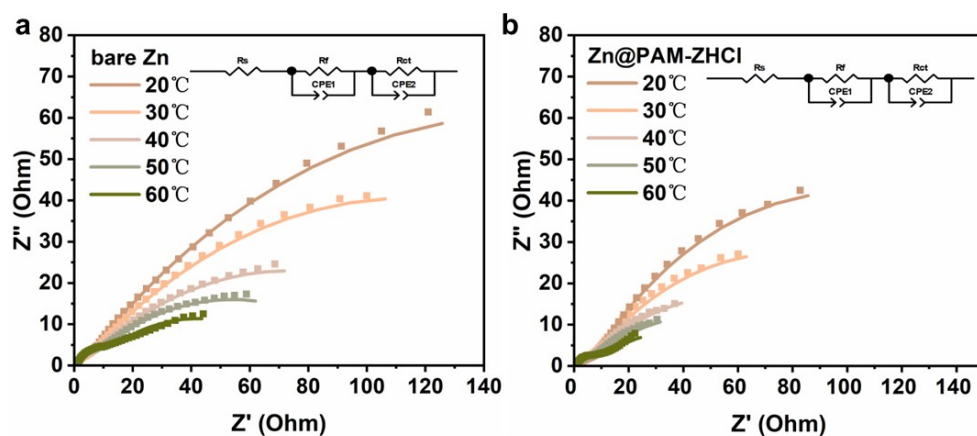


Fig. S19 EIS curves of the (a) bare Zn and (b) Zn@ PAM-ZHCl at different temperatures.

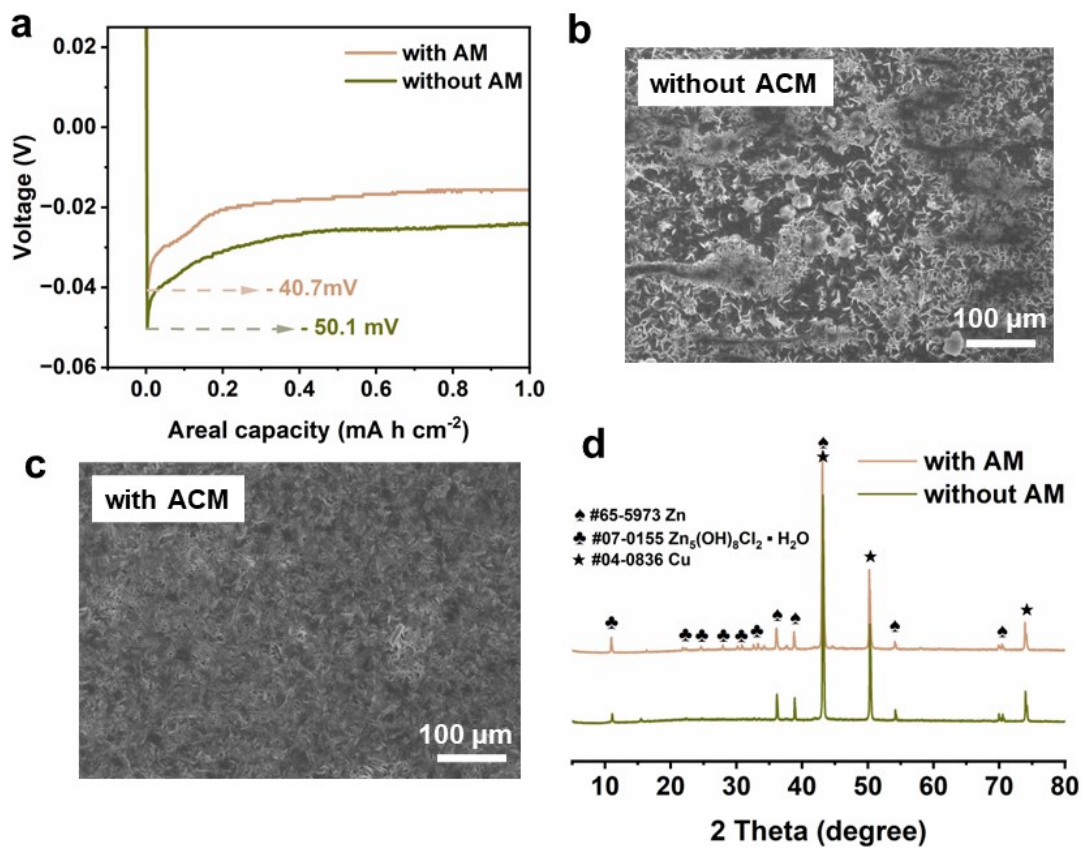


Fig. S20 (a) Initial deposition voltage profile. SEM images of the Cu foil at stripping state (b) without AM additive (c) with AM additive. (d) The XRD patterns of Cu foil without and with AM additive.

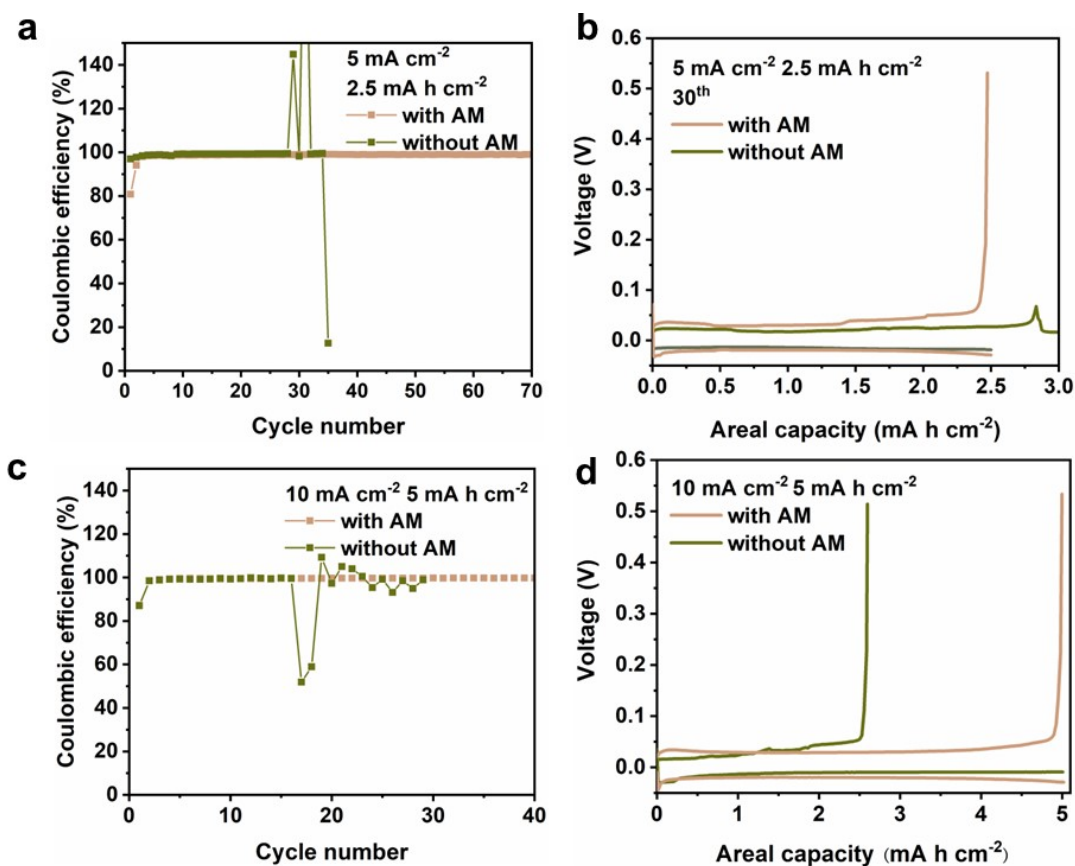


Fig. S21 The CE of the Zn//Cu asymmetric cells with and without AM additive (a) at 5 mA cm⁻² and 2.5 mA h cm⁻², and (b) the corresponding voltage profiles. The CE of the Zn//Cu asymmetric cells with and without AM additive (c) at 10 mA cm⁻² and 5 mA h cm⁻², and (d) the corresponding voltage profiles.

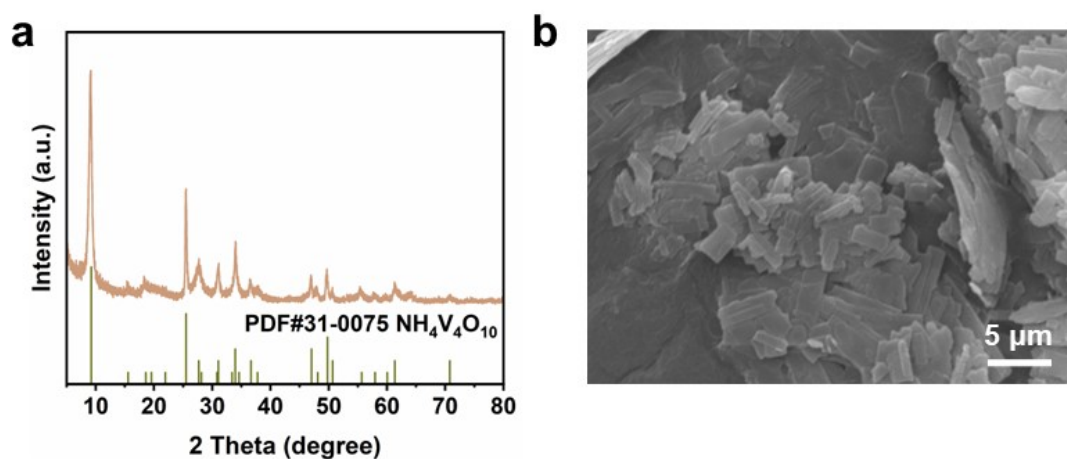


Fig. S22 (a) The XRD pattern and (b) the SEM image of NVO powder.

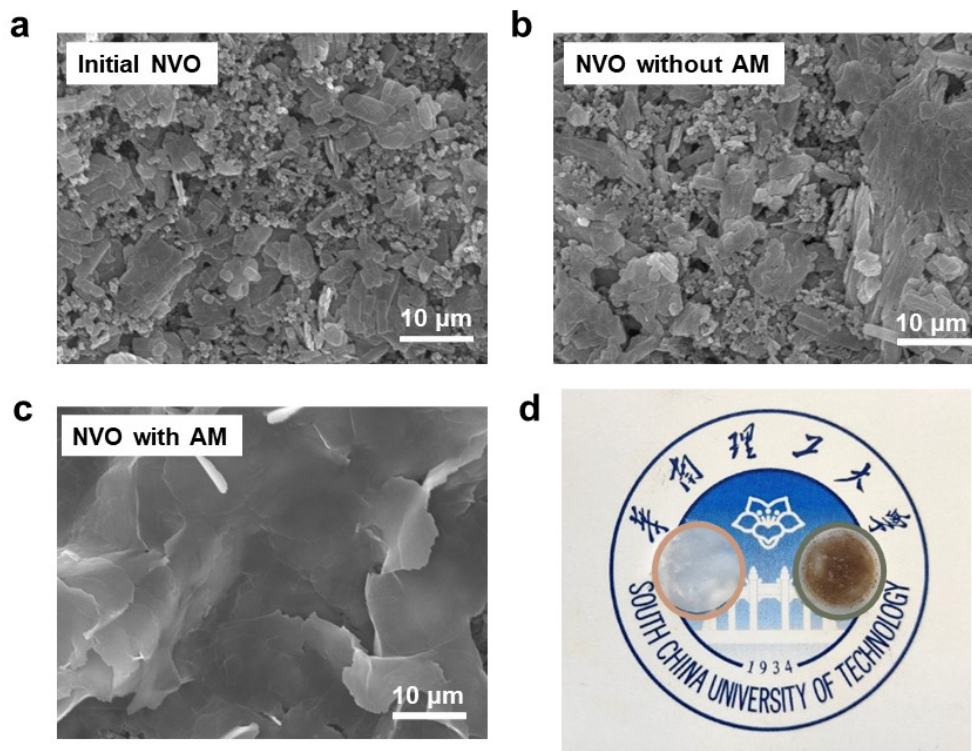


Fig. S23 (a) The SEM image of initial NVO cathode. The SEM image of NVO cathode after 50 cycles at 1 A g⁻¹ (b) without and (c) with AM. (d) Optical photograph of separators with AM additive (left) and without AM additive (right).

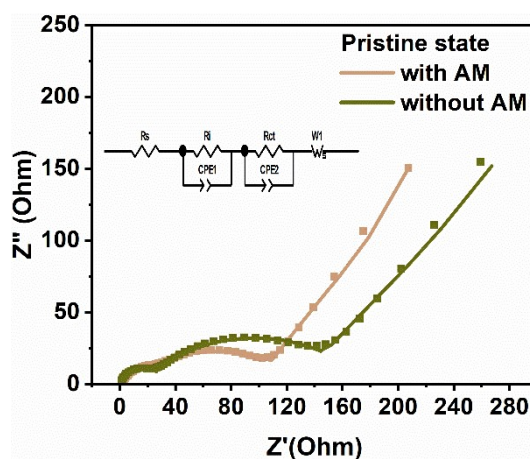


Fig. S24 The EIS curves of Zn/NVO cell at pristine state.

Table S2 the results of equivalent circuit fitting

pristine state			after cycling 50 th		
	Without AM	With AM		Without AM	With AM
R _s	1.15 Ω	1.24 Ω	R _s	1.29 Ω	1.85 Ω
R _i	33.25 Ω	23.01 Ω			
R _{ct}	128.90 Ω	82.67 Ω	R _{ct}	1.77 Ω	25.02 Ω

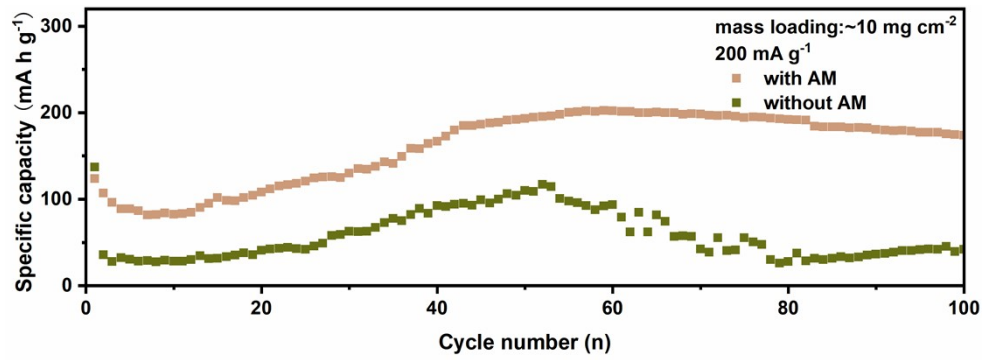


Fig. S25 The cycling performance of Zn//NVO cells with and without AM additive with high mass loading of the cathode at 200 mA g⁻¹.

References

- 1 G. Kresse and J. Furthmüller, *Comp. Mater. Sci.*, 1996, **6**, 15-50.
- 2 G. Kresse and J. Furthmüller, *Phys. Rev. B*, 1996, **54**, 11169-11186.
- 3 J. P. Perdew, K. Burke and M. Ernzerhof, *Phys. Rev. Lett.*, 1996, **77**, 3865-3868.
- 4 G. Kresse and D. Joubert, *Phys. Rev. B*, 1999, **59**, 1758-1775.
- 5 P. E. Blöchl, *Phys. Rev. B*, 1994, **50**, 17953-17979.
- 6 K. Qi, W. Zhu, X. Zhang, M. Liu, H. Ao, X. Wu and Y. Zhu, *ACS nano*, 2022, **16**, 9461-9471.
- 7 Q. Yang, L. Li, T. Hussain, D. Wang, L. Hui, Y. Guo, G. Liang, X. Li, Z. Chen, Z. Huang, Y. Li, Y. Xue, Z. Zuo, J. Qiu, Y. Li and C. Zhi, *Angew. Chem. Int. Ed.*, 2022, **61**, e202112304.
- 8 H. Qin, W. Kuang, N. Hu, X. Zhong, D. Huang, F. Shen, Z. Wei, Y. Huang, J. Xu and H. He, *Adv. Funct. Mater.*, 2022, **32**, 2206695.
- 9 Q. Li, A. Chen, D. Wang, Y. Zhao, X. Wang, J. Xu, B. Xiong and C. Zhi, *Nat. Commun.* 2022, **13**, 3699.
- 10 Y. Guo, W. Cai, Y. Lin, Y. Zhang, S. Luo, K. Huang, H. Wu and Y. Zhang, *Energy Storage Mater.*, 2022, **50**, 580-588.
- 11 H. Lu, X. Zhang, M. Luo, K. Cao, Y. Lu, B. B. Xu, H. Pan, K. Tao and Y. Jiang, *Adv. Funct. Mater.*, 2021, **31**, 2103514.
- 12 J. Ruan, D. Ma, K. Ouyang, S. Shen, M. Yang, Y. Wang, J. Zhao, H. Mi and P. Zhang, *Nano-Micro Lett.*, 2023, **15**, 37.
- 13 H. Wang, W. Ye, B. Yin, K. Wang, M. S. Riaz, B.-B. Xie, Y. Zhong and Y. Hu, *Angew. Chem. Int. Ed.*, 2023, **62**, e202218872.
- 14 M. Zhu, Q. Ran, H. Huang, Y. Xie, M. Zhong, G. Lu, F.-Q. Bai, X.-Y. Lang, X. Jia and D. Chao, *Nano-Micro Lett.*, 2022, **14**, 219.
- 15 K. Wang, T. Qiu, L. Lin, X.-X. Liu and X. Sun, *Energy Storage Mater.*, 2023, **54**, 366-373.
- 16 K. Guan, L. Tao, R. Yang, H. Zhang, N. Wang, H. Wan, J. Cui, J. Zhang, H. Wang and H. Wang, *Adv. Energy Mater.*, 2022, **12**, 2103557.
- 17 A. Naveed, G. Li, A. Ali, M. Li, T. Wan, M. Hassan, X. Wang, P. Ye, X. Li, Y. Zhou, M. Su, R. Guo, Y. Liu, H. Xu and D. Chu, *Nano Energy*, 2023, **107**, 108175.
- 18 J. He, Y. Tang, G. Liu, H. Li, M. Ye, Y. Zhang, Q. Yang, X. Liu and C. Li, *Adv. Energy Mater.*, 2022, **12**, 2202661.